Evolution of Biological Eye in Computer Simulation

Neil Vaughan
Department of Computer Science
Digital Biology Research Group
University of Chester
Chester, United Kingdom
n.vaughan@chester.ac.uk

Abstract—**This research demonstrates an evolutionary process of a biological eye in a computer model. This demonstrates using a model, how the biological eye could have evolved, starting from a sheet of light sensitive cells towards a concave pinhole camera eye without a lens. The advantages of each iterative improvement lead to increased chance of being selected for subsequent generations because improved eye clarity helps animals to detect prey or predators. The fitness of the evolving eyes are evaluated on a range of 5 varied datasets with a range of classification algorithm tasks. The developed simulated eye model demonstrates that the requirement to detect the direction of an approaching predator does produce a gradual evolutionary transition from a flat light sensitive surface to the pinhole camera eye which models how eyes evolved in biological creatures.**

Keywords—eye, evolution, vision, simulated

I. Introduction

This research applies computer simulations aiming to reveal the evolutionary process of the eye.

Darwin claimed that it seemed absurd to propose that the eye evolved through natural selection. Eye evolution has been labelled as Darwin's Greatest Challenge (ScienceDaily, 2004). This is because the eye contains so many complex interacting parts. There are numerous parts to an eye that appear to be dependent on each other which has long been regarded as a scientific conundrum:

1) Physical mechanism (retina). The physical eye shape evolves to capture light rays and put them onto a flat retina.

2) Optimisation of the mechanism (lens). The lens shape evolves simultaneously to improve clarity, reducing blur.

3) Neural network. Biological brains to process the images for image classification have to evolve in parallel.

Biologists and creationists have historically disagreed over the evidence for the evolution of biological eyes (Dawkins, 1986). Views opposing evolution claim that if any part was missing, the whole eye could not function and would be rendered useless, therefore all parts of the eye must be present and incremental gains of 1% or 2% of an eye would be meaningless. Biological evolution cannot easily be observed (as it occurs over geological timescales), or recreated in a laboratory. The fossil record scarcely captures evidence to demonstrate eye evolution because the eye is primarily soft tissue. However evolution of the eye in trilobites has been studied (Clarkson, 1975).

There are many animals alive today acting as living fossils, with eyes in various stages of development from simple light detecting cells, to basic pinhole camera type eyes and more advanced lens based eyes. Birds of prey and hawks in particular have excellent long-distance vision. The conventional stages of eye evolution includes a number of milestones: (1) Eye evolution begins from introduction of a simple flat retina or piece of light sensitive skin, which in itself is far more useful than no eye, enabling detection of day or night and shadows of approaching predators, perhaps even colour differentiation. (2) A flat retina would evolve into a light sensitive cup of increasing depth, which has the benefit of detecting the direction of shadows perhaps from a predator or prey, without requiring a focussed image. (3) Next would be a concave ever deepening crescent which is better at estimating directions and the sides begin to curve inwards forming a thinner opening. (4) What follows as the opening narrows is a more precise pin-hole camera without lens as found on the octopus which precisely focusses the image. (5) Finally a lens would evolve, which could begin with any lump of misshapen translucent tissue which would offer some focal benefit before evolving into an optimised lens shape. This research develops a computer simulation model presenting evidence for this complete hypothesis of eye evolution.

Darkness and camouflage make it harder for creatures to see things. This is an important crux of the mechanism for eye evolution. Dusk and nightfall could make the difference whereby an eye 1% better, would be just capable of identifying camouflaged prey at dusk, whereas the 1% worse eye could only identify it just before dusk. This model investigates effects of brightness for performance evaluation of pinhole camera eyes.

B. Related work

A model for the evolution of the eye was presented by Nilsson & Pelger (1994). This was widely circulated and referred to as important evidence for Darwin’s theory of evolution including by Richard Dawkins on televised Christmas lectures in 1991. However Nilsson & Pelger’s model was controversially criticised by Berlinksi (2003), because it didn’t contain any computer simulation model as suggested, which rendered their arguments trivial and their conclusions unsubstantiated. Rhodes (2007) agreed the Nilsson & Pelger model to be at least five times to an order of magnitude too small.

Simulating the evolution of the eye can enable many real world applications and uses. For example, eyes have been evolved in robot hardware by adjusting angles of light sensors (Lichtensteiger & Salomon, 2000). Evolution was shown capable of optimising the 3D structure of lenses which can focus light rays onto a point by Hotz (2004) using either direct or developmental indirect encodings.

Simulation has been used to estimate the time taken for eyes to evolve in spiders (Williams, 2011). More recently, Machado *et al.* (2017) claim to produce the first computer simulation models of eye evolution using genetic algorithms. However these are basic models, whereby each eye is represented by just a 3x3 array of Boolean values, considering no physiological attributes. Fitness of each eye was calculated by applying arbitrary penalties defined by the authors. This does not appear to demonstrate sufficient details about eye image generation or fitness evaluation to represent biological processes.

Experiments showed that genes controlling development of the eye can be traced back to Cyanobacteria which do not have multicellular retina (Gehring, 2005).

II. METHODS

A. Model setup

This research presents a 3D model of the eye simulating individual light rays from external objects onto the retina. Simulations use ray-casting to simulate what the eye would see as it evolves, detecting objects with different quality images to demonstrate that gradual 1% increments to eye quality are beneficial (Dawkins, 1986).

B. Simulating pinhole camera eye with curved retina

A novel method for modelling the 3D eye structure is generated by fitting a plane which is overlapped by a sphere with adjustable depth (Fig. 1). Using this simple representation the eye evolution is represented by the sphere moving forwards or backwards in one dimension to overlap the plane to various extents. The shape of the eye is the shape of the plane, which deforms to fit any part of the sphere which overlaps to its right. The sphere serves only to calculate how the plane deforms.

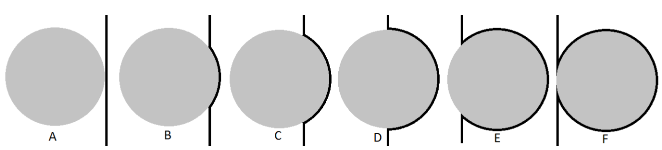

Fig. 1. Curved retina aye evolution modelled in 3D as a sphere overlapping a plane.

Initially, the eye begins as a flat light sensitive area (Fig. 1A). As the sphere moves below the plane, it creates a shallow eye cavity (Fig. 1B). As the sphere overlaps further, this creates a larger depression of increasing depth (Fig. 1C). As the sphere progresses it becomes a hemisphere at which point the opening reaches maximum size of *2r* where *r* is the radius of the sphere (Fig. 1D) As the sphere moves deeper still, the opening begins to narrow (Fig. 1E). Finally, the pinhole begins to form and decreases rapidly in size as the sphere approaches the limit of depth *2r* and pinhole size approaches towards 0 (Fig. 1F).

Each eye at a particular stage of evolutionary development, such as those in Fig. 1A-F is a phenotype. All information required to re-create the phenotype is stored in a genotype which changes each generation by mutations and evolution. The genotype in this model is simply the sphere depth *d*, the distance by which the sphere overlaps the plane.

Pinhole diameter p can be calculated from the sphere depth d by Eq. 1 which shows that for any sphere of radius r, in this case r=10mm, when sphere depth d ranges from 0 to $2r$, the pinhole diameter p also ranges from 0 to $2r$. The eye was generated as a 3D CAD model, shown in Fig. 2

$$p = \sin\left(\left(\left(\frac{d}{2r}\right) * 180\right) * \left(\frac{\pi}{180}\right)\right) * 2r \qquad (1)$$

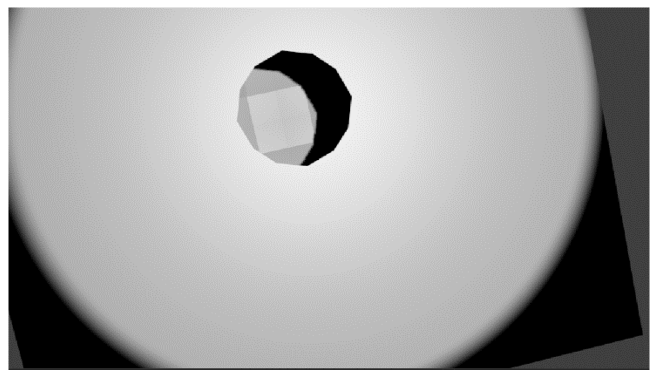

Fig. 2. Computer CAD model of a 3D pinhole eye based on defined model.

The amount of light δ passing through a pinhole, is proportional to the number of rays passing through a pinhole which is proportional to the area of the pinhole A and brightness of light source b, such that $\delta=Ab$. It follows that the amount of light δ can be calculated in relation to the pinhole diameter p by Eq. 2**.**

$$\delta = \frac{\pi}{4}p^2 \qquad (2)$$

C. Evaluating fitness of each eye

The next step is to evaluate the fitness of each eye to select for the next generation. Scoring is achieved by evaluating the images the eye observes. Image quality evaluation is achieved by conducting a series of classification tasks using the images observed from the eye. The hypothesis is that classification accuracy is dependent on high quality images. The eyes that see more clearly are identified by an improvement of image classification accuracy. If one creature's eyes are subtly able to see more clearly, that small difference could enable it to classify a passing object as either a predator or prey, increasing the creature's fitness and chances of survival. The next sections describe the steps that are completed for each eye to evaluate its fitness.

D. Datasets

Well-known datasets were obtained and new datasets fabricated to provide images and 3D scenery that were observed by the evolving eyes. Five separate datasets were each tested. (1) The well-known data science *owl vs butterfly* dataset was used containing 100 images in two classes. (2) A much larger 25000 image two-class dataset of *cats and dogs*. (3) A custom made 3D VR scene of a forest of trees, some images contain a wolf and fox. (4) Images of group photos with human faces using face detection algorithm. (5) A set of custom binary datasets each with 800 images containing a predator approaching from either left or right and with a predator either present or not. This final dataset proved most useful and was used in most detail, shown in Fig. 3 and section E.

E. Custom made Left-right and present-not datasets

When predators or prey approach, a creature's chance of survival increases with its ability to identify the direction of approach. Creatures evolve to detect predators. If a predator is present and the eye cannot detect it, the creature isn't selected for the next generation because it would die if it doesn't protect itself. This new dataset was generated specifically to facilitate evaluation of left vs right classification. The dataset contains 800 images. All images contain a predator, 400 are on the left and 400 are on the right. The predators are random sizes, small and big are both included to represent various distances and visibilities. All backgrounds are green. The colour of predators is always red, but the amount of red being added to the predator varies from 6%-50%, to represent camouflage. The random colour and random size were included to provide training examples representing difficult to see and camouflaged hiding predators. Circles were either in the left 1/3 of the image or the right 1/3, never the central 1/3, which avoids uncertainty. The center of each predator's position was restricted to within a fixed distance from the center of the image, to prevent predators in the far corners which could be distorted by a pinhole eye.

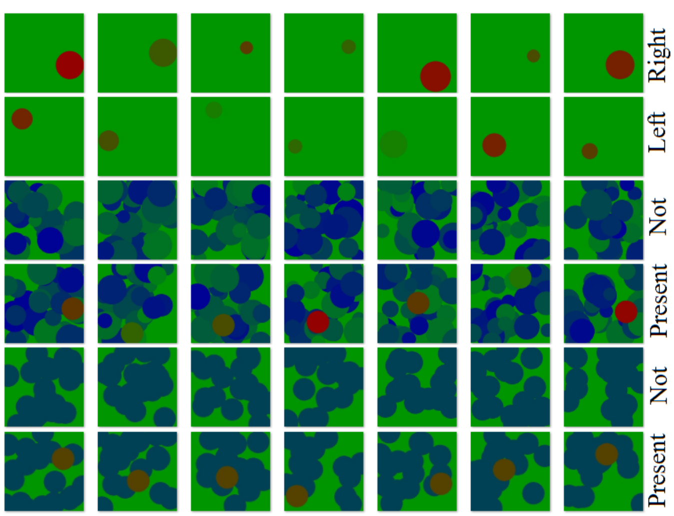

Fig. 3. Parts of the generated datasets left-right and present-not. Red circles represent predators to be detected by the classification algorithms.

All datasets provided binary classification tasks. Each dataset was subsequently converted to produce sets of images which are as would be seen by 20 eyes spanning the complete range of pinhole sizes from a flat light sensitive skin, to a small pinhole pre-processed and classified using the same process shown in the next sections.

F. Generating the eye's view images

For each of the 5 datasets the 3D eye computer model is used to generate the set of 800 images for each of the 20 eyes ranging from 0 to 19 mm in 1mm incremental steps, under 4 light conditions demonstrating comprehensive examples of the view that each particular eye would see.

At each stage of eye evolution the model can simulate what would be seen on the retina, by using ray tracing to identify which parts of the virtual environment are visible to each light cell on the simulated retina.

G. Raycasting algorithms

Ray-casting is used to project images on the retina based on the light rays individually passing through the pinhole from the object of interest being observed.

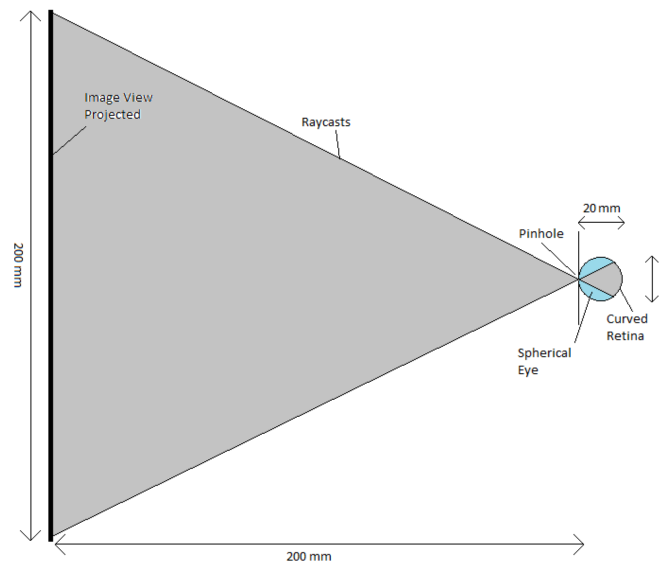

Fig. 4. Scaled model of the virtual pinhole eye model raycasting.

Collision detection and path of light rays is individually calculated accordingly to the 3D model which consists of a sphere and cube. If a light ray is (1) outside of the frontal plane of external skin or is (2) within a 3D Euclidean distance of r from the center of the sphere, where r is the radius of the sphere, then the light ray has not collided. When a light ray collides with the retina surface, the algorithm identifies which light sensitive cell will detect that ray based on the closest cell to the impact location.

H. Ray-casting algorithm - planar

The planar ray-casting pinhole camera eye is defined by Eq. 3. The process starts by identifying where on the retina each ray cast will land: For each pixel s in the scene S, cast a ray through each pixel p in the pinhole P. The retina pixel that the light ray hits is at position r' which is equal to the position of this pinhole pixel p' plus the difference between the pinhole pixel p' and the scene pixel s' multiplied by d. d is the ratio of the distances between pinhole pixel p' and the retina pixel r' divided by the distance between the pinhole pixel p' to scene pixel s'.

$$\sum_{s=1}^{S}\sum_{p=1}^{P} r' = p' + (p' - s') * d \qquad (3)$$

```
For each pixel in image{
  For each pixel in pinhole.{
    //ray-casting
    projx = pinx + (float)(pinx - origx)*(float)((float)pintoret /
(float)imgtopin);

    //collision detection
    if (projx >= 0 && projx<image_orig.cols && projy >= 0
&& projy<image_orig.rows)
}}
```

The rays are then divided to take the average light on each retina cell:

```
For each pixel in retina{
  Retinacall(I,j)= Retinacall(I,j) / maxexposure
}
```

The pinhole camera produces an image on the retina (Fig. 5) which has various expected properties: (1) rotated 180 degrees (2) blur is proportional to the pinhole size and (3) image size is proportional to the ratio of distances between the object – pinhole and the pinhole – retina.

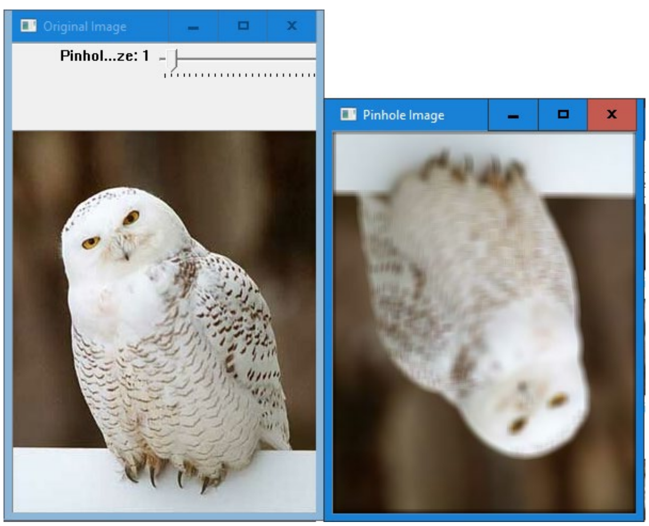

Fig. 5. View of a snowy owl (Bubo scandiacus) through an evolved simulated 5-pixel pinhole camera eye (custom developed eye evolution software).

A more advanced realistic curved retina model was further developed and results demonstrated in Fig. 9. These are the steps for computing the spherical retina with circular pinhole:

1. calculate the 3D location of points on sphere surface.
2. calculate the 3D location of points on pinhole circle.
3. cast rays - check where the lines intersect 3D plane.
4. convert the points from sphere into a 2d array.

I. *Varying the light conditions*

Within the 3D VR scene, the light sources were reduced and in the other datasets, which resulted in reducing the brightness on each image to -50%, -85% and -95% (Figs. 6 & 7). In this algorithm brightness is adjusted in each image and 3D scene environment, which is expected to consistently reduce the ability of the algorithms to achieve classification of darkened images. Because the predators and prey are rather large, it is unclear whether very accurate eyes are beneficial over basic eyes. Therefore, for each eye, each scenario is modified into differing lighting conditions.

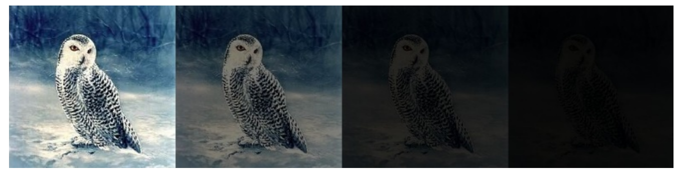

Fig. 6. A snowy owl (from owl vs butterfly dataset) viewed in different lighting conditions (a) Daylight, (b) -50% lighting, (c) -85% lighting, (d) -95% lighting. Classification of the owl becomes more difficult as light reduces. An eye with 1% improvement may prove more capable in dusk conditions.

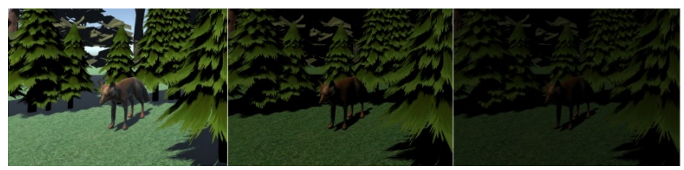

Fig. 7. The developed VR 3D Scene of a spruce forest containing predators at various light levels. This provides one of the custom fabricated datasets for image classification to evaluate the evolving eyes.

J. *Pre-processing filter*

The total of 1600 images were pre-processed to extract image features using ColourLayout filter algorithm and EdgeFilter algorithm both were tested.

Firstly, pre-processing filters are applied to the raw images. That extracts additional numerical features from the images which can be used to classify. Various pre-processing filters were tested including Fuzzy Opponent Histogram, Binary Patterns Pyramid, Edge Histogram and Colour Layout filters. These were applied to provide capability for animals to be classified either by their colours or by presence of edges.

K. *Classification algorithms*

Classification was applied to the resulting 800 processed images for each of the 20 eyes. To assess the eye image quality precisely, 16 different classification algorithms were applied to each including (1) decision trees: J48 and random forest, multi-layer perceptron neural networks, stochastic gradient descent (SGD). Face recognition algorithm to detect faces in images with people. This variety of classification methods ensured that the results were not biased by a feature of one particular classification algorithm.

L. *Evolutionary algorithm*

The eye begins as a flat piece of light sensitive skin. All images from each dataset are then passed into the eye model which generates the images that the eye would see. The resulting eye-view images are evaluated to quantify the performance of the eye using classification algorithms. Genetic parameters are randomly mutated to re-generate a new 3D eye model. The evaluation of the new eye is conducted. The performance of the new eye and the previous eye are then compared, and only the fittest of these two is used to generate the subsequent eye.

III. Results

A. Face detection:

One approach that was tested to assess the eye fitness was to apply an algorithm for face detection. If the eye captures a blurred image, face detection works less well (Fig. 8.). This quantifies a fitness for each eye and the eye would evolve to be less blurred to improve fitness and face detection. However, for very low quality eyes, such as flat pieces of light sensitive skin in early eyes, face detection will never work because there is no evolutionary trajectory.

This has shown that face detection accuracy could be useful as part of a fitness function to evolve the eye mechanism which controls the clarity of the images. However it is only mainly useful for fine-tuning eye evolution, because any significant amount of blur causes face detection algorithms to fail entirely and detect no faces, in which case the evolutionary trajectory would not be present in the early stages of evolution from basic light sensitive cells.

Fig. 8. When eyes evolve clarity and reduce blur, the performance of face detection algorithms improve. Smaller faces further from camera require most clarity.

B. Brightness reduction

Adjusting the brightness of each image didn't consistently reduce the ability of the algorithms to achieve classification. In some cases, counterintuitively, reducing brightness by 85% improved classification accuracy. It was expected that reduced brightness could represent nightfall introducing difficulty in seeing things, but apparently the edges and colours still persisted, enabling classification in low light conditions (Table 1).

TABLE I. Table 1. Percentage classification accuracy with various pre-processing filters was not consistently affected by brightness reduction.

Brightness reduction	Colour Layout filters	Edge Histogram	Binary Patterns Pyramid	Fuzzy Opponent Histogram
0%	90	79	79	79
50%	93	78	77	70
85%	86	83	50	79
95%	91	50	50	80

C. Curved Retina Results for Owl vs Butterfly

Results showed a gradual tendency to increase classification accuracy as pinhole size and blur decrease. However the effect may be more if the pinhole size was increased faster, or in fact if the image classification didn't rely so much on colour, as owl and butterfly are very different colours in this sample dataset

Fig. 9. View of 4 owls and 2 butterflies through curved retina pinhole eye at 10 stages of eye evolution.

TABLE II. TABLE 1: ACCURACY FOR J48 CLASSIFICATION ALGORITHM APPLIED TO OWL VS BUTTERFLY DATASET WITH FLAT RETINA PINHOLE EYE.

Sphere Depth (mm)	Pinhole Diameter	Pinhole Area (mm^2)	Colour Layout	Edge Histogram	Binary patterns	JPEG coefficient	PCTH	Mean
19.90	0.31	0.08	88	86	74	87	91	85.2
19.85	0.47	0.17	86	93	65	94	89	85.4
19.80	0.63	0.31	86	79	65	93	92	83
19.75	0.79	0.48	90	78	67	95	93	84.6
19.70	0.94	0.70	89	74	70	97	92	84.4
19.65	1.10	0.95	84	78	72	94	94	84.4
19.60	1.26	1.24	83	78	66	97	95	83.8
19.55	1.41	1.57	88	67	60	93	95	80.6
19.50	1.57	1.93	90	58	75	91	96	82
19.45	1.73	2.34	90	66	70	90	92	81.6

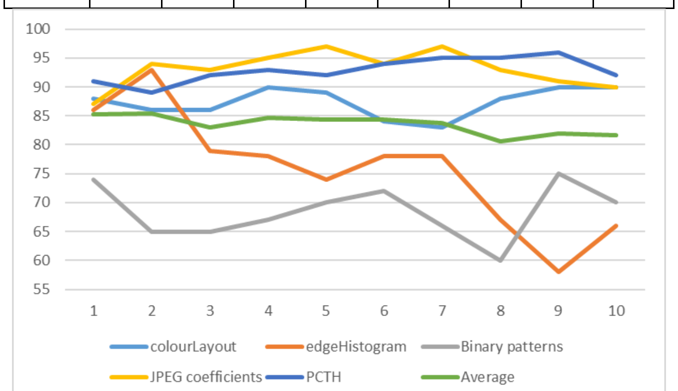

Fig. 10. Fine tuning the small pinhole: shows increasing pinhole diameter, related to more blur. Y axis is classification accuracy. X axis shows 10 different pinhole sizes.

D. Results from left-or-right dataset classification.

When a predator or prey approaches it is useful to detect the direction of approach. This can't be done with flat skin and improves with depth of the concave depression. The left-right dataset (Fig. 3 top two rows) produced a smooth evolutionary trajectory demonstrating evolution from flat light sensitive skin to pinhole eye. At all stages of evolution, there are some circles just faint enough to be a challenge for each stage of eye.

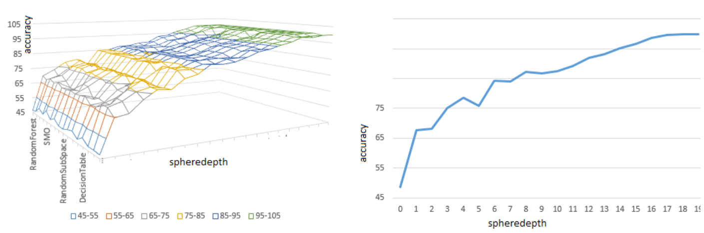

Fig. 11. The task of distinguishing left from right does cause an evolutionary gradient to be present for all depths of pinhole eye from flat skin to precise pinhole. (a) 16 different classification algorithms. (b) the mean classification accuracy as the pinhole eye evolves smaller.

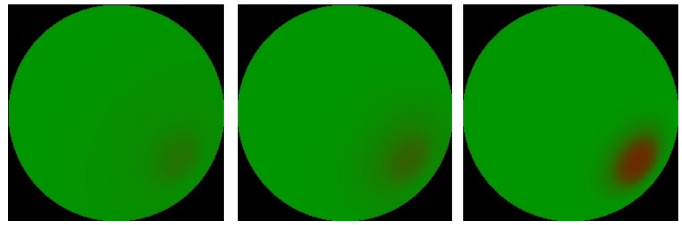

Fig. 12. One example from the left-right dataset as seen through 3 curved retina eyes at various stages of pinhole size evolution showing improved clarity as pinhole reduces from (left) 9mm, (middle) 6mm, (right) 3mm.

E. Results from left – right with no random colours or sizes.

This dataset produced no evolutionary trajectory. This differs from the previous left-right dataset because the predators are all the same size and colour which represents no camouflage or difficult borderline cases. Comparing these two left-right and left-right-no colours datasets, shows that in order for an evolutionary trajectory to be present, the task needs to be of mixed difficulties by including some easy to classify and some hard to classify examples (which only the finest pinholes can detect). Without this mixture of difficulties, the evolutionary trajectory isn't present and increasing the pinhole eye clarity isn't always beneficial.

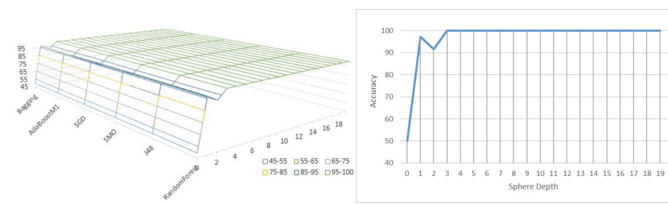

Fig. 13. When the task is easier, because no smaller sizes and no reduced colours are present, there is no evolutionary trajectory.

F. Results from Present-or-not dataset

This present-or-not dataset contained a plain green background with circles all the same size and colour.

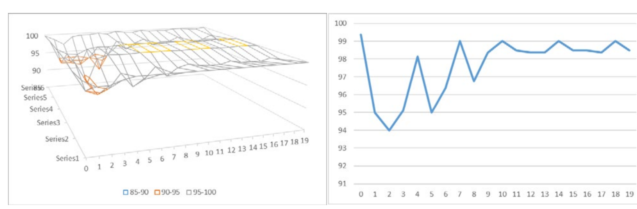

Fig. 14. This result shows that there is no trajectory present for present or not. The 0 spheredepth is already able to classify extremely well, and no further improvement is made by improving the pinhole and spheredepth. A future work could check perhaps introducing tiny or extremely camoflagued objects may introduce a trajectory.

G. Results from Present or not dataset with structured background

In this dataset, all predators were red circles of the same size and same colour. The background had random blue circles of different sizes and shade (Fig. 3, bottom two rows).

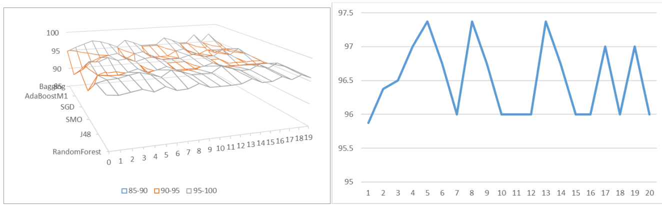

Fig. 15. Shows that there is no trajectory when classifying present or not even with different coloured random backgrounds, it almost perfectly scores each time from depth 0.

H. *Results from present-not-structuredback+random*

In this dataset, predators were red circles with slightly random colour but not random sizes. Background contained random blue circles. (Fig. 3, middle two rows). There was no evolutionary trajectory in this dataset, and the classifiers achieved around 90% accuracy with almost all pinhole sizes. This dataset did not contain mixture of predator sizes, retesting with random sizes could potentially produce interesting results.

I. *Lens evolution*

Future research could investigate the evolution of a ray-casting lens. However, in order for a pinhole eye to evolve a lens the pinhole must grow in size, losing accuracy, before the option of fitting a lens is possible (Rhodes, 2007).

IV. Conclusion

This research has demonstrated that for the eye to evolve, it is critical for the evaluation task (fitness function) to include objects of random colours and sizes, which introduced a mixture of difficulties, some of which can only be solved with the keenest eye. In datasets where all objects are the same size, no evolution occurs. This confirms Dawkins (1986) suggestions that camouflage, low light, and occlusion are important to explain the benefits of 1% incremental improvements during the evolution of the eye.

It was expected that the graphs produced would always contain some noise. These graphs were generated in 1mm steps, but in future it could be repeated with 0.5mm steps. Also noise can come from the particular properties of this dataset or this implementation of code, further tests on larger datasets would produce even smoother graphs, if required, although these present graphs are sufficient to demonstrate beyond doubt the presence and absence of evolutionary trajectories.

Evolutionary trajectory was demonstrated from flat skin to pinhole eye. It starts with the task of detecting a predator. A dataset was created with 2 classes, in which a red object (predator) was either present, or not present. The classification was almost perfect with a flat light sensitive skin, and this task alone had no evolutionary trajectory to evolve further into concave skin or a pinhole. The next skill is to detect the direction of a predator. Detecting direction was impossible with flat skin, classification scores just 50% - no more than chance. With a tiny concave surface of depth 1 was impressively 65% accurate at determining predator direction. This produced an evolutionary trajectory to be present as accuracy gradually increased up to a hemisphere eye. Finally, the eye is fine-tuned by more sophisticated tasks such as detecting faces. The face detection dataset demonstrated the evolutionary trajectory from hemisphere eye to pinhole eye, showing that a high-level task like face detection requiring precise accuracy can be used as part of the fine tuning for a fitness function to evolve the eye mechanism which controls the fine clarity of the images. Overall, no individual classification task alone created an evolutionary trajectory from flat skin to perfect pinhole eye. But living in a structured environment, many mixed types of classification would be required combining several trajectories.

The task of detecting and classifying animals is a valid fitness function for evolution of eyes since that is what would enable biological predators and prey to survive and reproduce. The classification accuracy was shown to produce an evolutionary trajectory which demonstrates how Darwinian evolution with random mutations could lead to the production of a pinhole camera eye, starting from a flat piece of light sensitive skin in 1% increments.

Acknowledgment

The Royal Academy of Engineering (London, UK) have contributed and supported this research through a Research Fellowship awarded to Dr Neil Vaughan.

References

[1] Dawkins, R., (1986) The blind watchmaker: Why the evidence of evolution reveals a universe without design. https://terebess.hu/keletkultinfo/The_Blind_Watchmaker.pdf

[2] Nilsson, D. E., Pelger, S. (1994) A pessimistic estimate of the time required for an eye to evolve, Proceedings: Biological Sciences, 256(1345), p 53-58. http://www.squarefree.com/mirrors/eye1.pdf

[3] Science Daily, (2004), https://www.sciencedaily.com/releases/2004/10/041030215105.htm [Accessed 2018].

[4] Lichtensteiger, L., & Salomon, R. (2000). The evolution of an artificial compound eye by using adaptive hardware. In Proc. of The 2000 Congress on Evolutionary Computation, p1144-1151. https://pdfs.semanticscholar.org/9d41/8397e65cbfc7b4ef11be403184a2c73d0f1a.pdf

[5] Machado, R. S., Castellanos, A., & Lahoz-Beltra, R. (2017) Eye evolution simulation with a genetic algorithm based on the hypothesis of Nilsson and Pelger. International Journal "Information Theories and Applications", 23(3), p221. http://www.foibg.com/ijita/vol24/ijita24-03-p02.pdf

[6] Darwin, C., (1859) On the origin of species by means of natural selection. London: John Murray.

[7] Berlinski, D. (2003). A scientific scandal?. Commentary, 116(1), 10.

[8] Rhodes D., (2007) Approximating the Evolution Time of the Eye: A Genetic Algorithms Approach, Thesis, Indiana University.

[9] Williams, V., (2011) Simulation for the Evolution of the Australian Netting Spider PM Eye. arXiv:1111.0977 [q-bio.PE].

[10] Hotz, P. E., (2004), Comparing direct and developmental encoding schemes in artificial evolution: A case study in evolving lens shapes. CEC (10.1109/CEC.2004.1330934).

[11] Clarkson, E. N. (1975). The evolution of the eye in trilobites. Fossils and strata, 4(7).

[12] Gehring, W. J. (2005). New perspectives on eye development and the evolution of eyes and photoreceptors. Journal of Heredity, 96(3), 171-184.